

Driver Cell Phone Usage Violation Detection using License Plate Recognition Camera Images

Bensu Alkan, Burak Balci, Alperen Elihos and Yusuf Artan

Video Analysis Group, Havelsan Incorporation. Ankara, Turkey

{balkan, bbalci, aelihos, yartan}@havelsan.com.tr

Keywords: Cell Phone Usage Detection, Convolutional Neural Network (CNN), Deep Learning, Object Detection, Traffic Enforcement, Intelligent Transportation Systems (ITS).

Abstract: The increased use of digital video and image processing technology has paved the way for extending the traffic enforcement applications to a wider range of violations as well as making the enforcement process more efficient. Automated traffic enforcement has mainly been applied towards speed and red light violations detection. In recent years, there has been an extension to other violation detection tasks such as seat-belt usage, tailgating and toll payment violations. In the recent years, automated driver cell phone usage violation detection methods have aroused considerable interest since it results in higher mortality rates than the intoxicated driving. In this study, we propose a novel automated technique towards driver's phone usage violation detection using deep learning algorithms. Using an existing license plate recognition camera system placed on an overhead gantry, installed on a highway, real world images are captured during day and night time. We performed experiments using more than 5900 real world images and achieved an overall accuracy of 90.8 % in the driver cell phone usage violation detection task.

1 INTRODUCTION

Modern cities stand on the edge of a transformational change that is driven by the technological innovation. Smart city technologies are revolutionizing the way we live, see and think the cities we live in. Thanks to the proliferation of sensors placed around the city, cities continuously collect data to monitor security and welfare of its citizens. Law enforcement agencies may also benefit from data streaming from these sensors. In the recent years, many companies have proposed smart law enforcement solutions using machine learning techniques towards traffic enforcement, predictive policing and crime prevention (IBM *report*, 2012).

Traffic enforcement on highways and roads is typically performed manually by a road-side police officer. However, this process is known to be laborious and ineffective due to the lack of sufficient personnel to perform the inspection. Therefore, there has been a need to develop automated systems that would assist police officers in the enforcement process. Camera based enforcement systems on roadways have been gaining popularity. Using the existing license plate recognition cameras that are installed for smart city purposes, we propose a driver

cell phone usage enforcement method using deep learning algorithms.

Although mobile phone usage while driving is prohibited in many countries, roadside surveys indicate that around 1% to 11% of drivers use phone while driving (ERSO *report*, 2015). In a recent study, the World Health Organization (WHO) reports that distracted driving (e.g. driver cell phone usage) results in higher mortality rates than that of intoxicated driving (WHO2017). Therefore, traffic safety agencies highly desire an automated cell phone usage violation detection system. Roadway surveillance camera images may offer an inexpensive and efficient solution to this problem (Artan et al., 2014; Berri et al., 2014; Seshadri et al., 2015; Le et al., 2016; Elings 2018).

Many studies in the past have proposed image based solutions towards traffic enforcement purposes. Most of these earlier studies present solutions towards seat belt detection, red-light violation detection, autonomous driving etc. to name a few (Zhou et al., 2017; Bojarski et al., 2016). In this study, we propose driver cell phone usage violation detection using license plate recognition camera images. Proposed method utilizes deep learning based object detection method in the subtasks of the cell phone violation

detection process; windshield region detection, driver detection and phone usage detection.

In the next section, we discuss previous works for our task. Section 3 presents the details of our methodology. Then, we report our experiments and results using real world images. Final section presents our conclusion.

2 RELATED WORKS

In this section, we review the previous studies that proposed solutions to detect cell phone usage while driving. These studies utilized machine learning and deep learning based methods in their analysis as shown in Table 1. Artan et al., (2014) captured near infrared (NIR) images by a highway transportation imaging system for detecting cell phone usage by drivers. Once the NIR images are acquired, they detect windshield of the vehicle and apply DPM base face detector within localized windshield region. Upon the detection of drivers' face, 3 locally aggregated descriptors BoW, VLAD and FV are used in image classification tasks. Berri et al., (2014) proposed an algorithm that can detect the use of cell phones by using the frontal camera mounted on the dashboard of a vehicle. They used machine learning based SVM classifier for classification stages. Seshadri et al., (2015) detect faces to check the presence of hands and cell phones. Challenging Strategic Highway Research Program (SHRP-2, 2006-2015) face view videos are utilized for a study of driving behaviour. Their approach is to first detect the drivers' face using Supervised Descent Method of (Xiong et al., 2013) and extract the left side and right side of the face region. Next, feature extraction techniques applied on these left/right side images, and these features are classified using Real Adaboost (Schapire et al., 1999) and SVM (Cortes et al., 1995) to detect cell phone usage.

In recent years, deep learning algorithms have shown to be the most effective method producing state-of-the-art results on many challenging application areas such as object detection, image recognition, speech processing (Zhou et al., 2017; Bojarski et al., 2016; Liu et al., 2016; Redmon et al., 2016; Ren et al., 2015; Huang et al., 2017). Le et al., (2016) present a deep learning based Multiple Scale Faster R-CNN approach to solve the problems of driver distraction monitoring and highway safety, namely, the hand on the wheel detection and the cell-phone usage detection. They used Vision for Intelligent Vehicles and Applications (VIVA) Hand Database (Das et al., 2015) and SHRP-2 dataset.

Results of this study show that it performs only very slightly better than regular Faster R-CNN (Ren et al., 2015). Elings, (2018) proposed a straightforward convolutional neural network approach and a various combination of phone, hand and face detection and hand classification were compared. It must be noted that each study utilized different training and testing data, so comparison of this studies may be misleading.

Table 1: Overview of the previous works.

Authors	Algorithm	Detected Objects	Placed
Artan et al. (2014)	Machine Learning	Windshield, Face	Overhead Gantry on Highways
Berri et al. (2014)	Machine Learning	Face	Inside of the Vehicle
Seshadri et al. (2015)	Machine Learning	Face	Inside of the Vehicle
Le et al. (2016)	Deep Learning	Face, hand, steering wheel	Inside of the Vehicle
Elings (2018)	Deep Learning	Face, Phone Pose, hand	Mounted above the highway

3 METHODOLOGY

In this section, we describe the details of the proposed solution for driver's cell-phone usage violation detection task. Proposed solution consists of 3-stages; windshield detection, driver region localization and phone usage violation detection. Steps of the proposed cell phone usage detection method is shown in Figure 1.



Figure 1: Steps of the proposed method. Left, middle and right column show License Plate Recognition Camera vehicle image, detected windshield region and detected driver region, respectively. Yellow rectangle shows the presence of cell phone usage within the driver region.

In this study, for object detection tasks, we utilize a popular deep learning based object detection technique, Single Shot Multi Box Detector (SSD) (Liu et al. 2016). General architecture of the SSD model can be seen in Figure 2. In terms of object

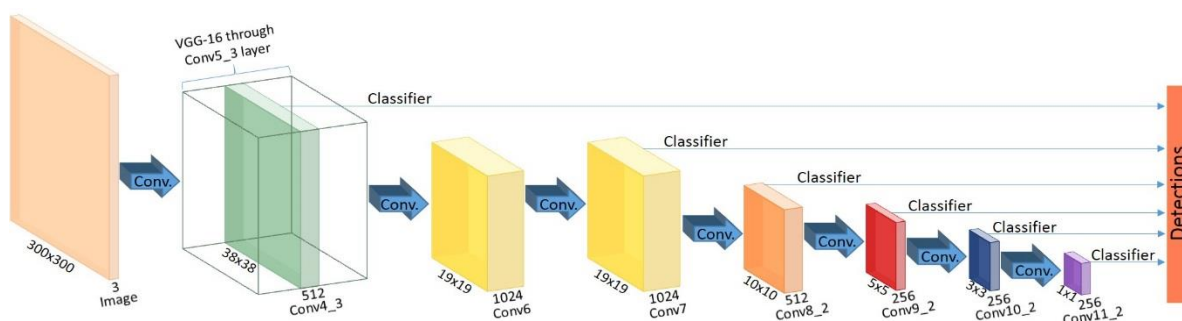


Figure 2: General architecture of SSD model (Liu et al., 2016).

detection tasks, SSD model is shown to perform better than alternatives (You Only Look Once (YOLO) (Redmon et al., 2016) and Faster R-CNN (Ren et al., 2015)) in terms of speed and accuracy (Huang et al., 2017).

3.1 Cell-Phone Usage Detection Stages

3.1.1 Windshield Region Detection

The first step in the violation detection task is the detection of the windshield region within the captured image. Windshield region constitutes the main region of interest (ROI) in phone usage detection task. Remaining part of the image is simply ignored since it is irrelevant for our objective. To construct windshield detector model, we fine-tuned a pre-trained SSD model using windshield region annotated training dataset. Afterwards, localized windshield region image is provided to driver and phone usage detection stages.

3.1.2 Driver Region Localization

Upon the completion of windshield detection, driver detection operation is performed within the detected windshield region. Driver detection is necessary since the image may contain undesired reflection effects due to environmental conditions. Driver detection allows us to eliminate the unnecessary violation detections in the images of windshield regions containing excessive amount of reflection. For driver detection model, we again fine-tuned a pre-trained SSD model using driver region annotated windshield images. At the end of this stage, localized driver region is given as input into the cell phone usage detection stage.

3.1.3 Cell Phone Usage Detection

Upon the completion of driver detection as described in earlier steps, we perform phone usage analysis on this localized driver region. Similar to windshield and driver detector models, we create another SSD model to capture the cell phone usage behaviour of driver. In our experiments, we compare the performance of proposed SSD object detection method with a convolutional neural network (CNN) and Fisher Vector (FV) based image classification methods for cell phone usage violation detection task as explained below.

3.2 Architecture of Proposed Methods

In this study, we utilized either an NIR image or RGB image in the decision making process. Instead of creating separate models for two types of image source, we convert single channel NIR images to 3 channel NIR images by cloning them channel-wise and generate a single model using NIR and RGB images together. Below, we explain training procedures and hyper parameter selections used in the training process.

3.2.1 SSD Model

In this approach, SSD object detector is utilized to detect the presence of a phone usage within the input image. To this end, we trained SSD model to detect phone usage violation in detected driver region. During the windshield, driver and phone usage detection training process, we utilized transfer learning approach to make the training process more efficient. We utilize a base SSD model presented in (Liu et al., 2016). Using this base model, we fine-tuned it with our specific dataset. Fine tuning operation is performed by freezing the weights of the first three convolutional blocks of the base model. The rationale behind this strategy is based on two

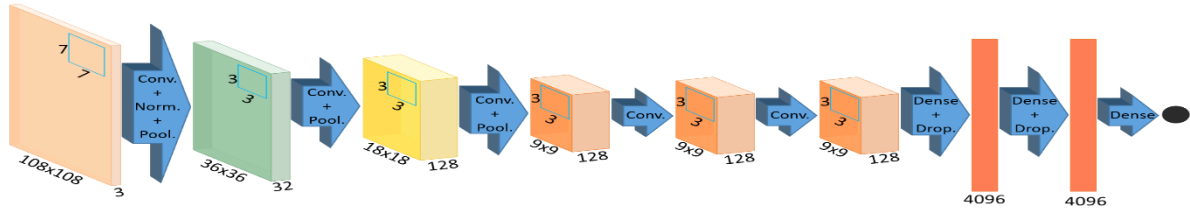


Figure 3: General architecture of CNN-P model.

facts. First three convolutional blocks trained with a large dataset (ImageNet-1k dataset (Deng et al., 2009)) behave as a feature extractor. Thus, there is no need to update these weights with our relatively small dataset. Secondly, since the first feature map to be analysed to detect objects fall into 4th convolutional block, it is logical to update weights starting from there. In our fine tuning operations, we set the batch size as 16. As learning hyper parameters, Adam optimizer (Kingma et al. 2014) with a relatively small learning rate 0.0003 is utilized. Also we applied learning rate decay strategy shown in Eq. 1 where λ is the learning rate, i is the epoch number.

$$\lambda_{i+1} = \lambda_i * 0.9^i \quad (1)$$

Using validation set, confidence threshold to accept detections as valid in windshield detection is determined as 0.95. Best performance is achieved with the confidence threshold of 0.8 in the driver detection and phone usage detection cases.

3.2.2 Convolutional Neural Network (CNN) Models

Very deep CNN models have achieved state-of-the-art performance in image classification tasks (Simonyan et al., 2014). In this study, we propose CNN based image classification. Proposed CNN architecture (CNN-P) is shown in Figure 3. In this architecture, the filter size of convolution layer 1 is chosen to be the same size as width of the phone usage within the image. Convolutional block of the model transforms input image to a 9x9x128 feature map. Then fully connected block works as a classifier to produce decision using feature map. All convolution and fully connected layers include rectified linear unit as an activation function. Cross entropy is used as loss function to train this model.

Since it is a small CNN model, we trained the model from scratch utilizing our dataset. Stochastic gradient descent (SGD) optimizer with learning rate 0.01 is utilized during the training. In order to avoid overfitting, the training was finished after 66th epoch.

3.2.3 Fisher Vector (FV) Model

Image vector representation using d -dimensional local image descriptors ubiquitously used in image classification studies. Suppose $\mathbf{X} = \{x_t, t = 1, \dots, T\}$ denote the set of T local descriptors extracted from a given image. We assume that the generation process of the local descriptors can be modelled by a probabilistic model $p(\mathbf{X}|\theta)$, where θ denotes the parameters of the function. (Perronnin et al., 2010) proposed to describe \mathbf{X} by the gradient vector;

$$G_{\theta}^{\mathbf{X}} = \frac{1}{T} \nabla_{\theta} \log p(\mathbf{X}|\theta) \quad (2)$$

In which the gradient of the log likelihood describes the contribution of the parameter θ to the generation process. A natural kernel on these gradient vectors is fisher kernel (Perronnin et al., 2010),

$$K(\mathbf{X}, \mathbf{Y}) = G_{\theta}^{\mathbf{X}T} F_{\theta}^{-1} G_{\theta}^{\mathbf{Y}} \quad (3)$$

where F_{θ}^{-1} denotes the Fisher Information Matrix of $p(\mathbf{X}|\theta)$. It is symmetric and positive definite, it also has a Cholesky decomposition $F_{\theta}^{-1} = L_{\theta}^T L_{\theta}$, therefore, the kernel $K(\mathbf{X}, \mathbf{Y})$ can be written as a dot product between normalized vectors shown in Eq. 4,

$$g_{\theta}^{\mathbf{X}} = L_{\theta} G_{\theta}^{\mathbf{X}} \quad (4)$$

where $g_{\theta}^{\mathbf{X}}$ is referred to as fisher vector of \mathbf{X} . Fisher vector extends the BoW by encoding first and second-order statistics. This description vector is the gradient of the samples likelihood with respect to the parameters of this distribution, scaled by the inverse square root of the Fisher Information Matrix. As a result, it gives a direction in parameter space into which the learned distribution should be modified to better fit the observed data. Therefore, FV describes the deviation of local descriptors from an average of descriptors that are modelled parametrically. In this study, FV is used as a method to capture the information conveyed by a set of descriptors into a fixed length representation.

In our experiments, we used Gaussian mixture models (GMM) with $K = \{32, 64, 128, 256, 512\}$ Gaussians to compute fisher vectors. The GMMs are trained using the maximum likelihood (ML) criterion

and expectation maximization algorithm (EM). Similar to (Perronnin et al., 2010), we apply power and L_2 normalization to fisher vectors to improve classification performance. In our experiments, we report results only for $K = 256$ since it achieved the best performance. For local image descriptors, we extract features from 32×32 pixel patches on regular grids at 3 scales. We only extract 128-D Scale-Invariant Feature Transform (SIFT) feature descriptors for these patches.

4 EXPERIMENTS

4.1 Image Acquisition

In this study, a 3MP (2048x1536) NIR and a 3MP (2048x1536) RGB camera pair with the same field of view (FOV) are placed on an overhead gantry approximately 4.5 m above the ground level. Video based triggering is used during the image acquisition. Figure 4 illustrates a camera directed at the windshield of the vehicle.



Figure 4: Visual illustration of image acquisition system.

4.2 Datasets

In the training process of the windshield, driver and phone usage detection stages, we utilized 768 (NIR+RGB) images to train models and 192 images were used for validation. Training dataset includes NIR and RGB images to be able to utilize models over both type of images. We have partitioned our training set into 3 classes; positive (violation), negative (no-violation) and hard negative which is shown in Figure 5.

For testing purpose, 2264 RGB images (2173 negative, 49 positive, 42 hard negative) and 3717 NIR images (3519 negative, 113 positive, 85 hard negative) were collected from various hours of a day. Positive and hard negative test images are relatively small from negative test images because of the difficulty in collecting data as a result of low



Figure 5: First, second and third column represent negative, hard negative and positive images, respectively. First row shows RGB sample images, second row illustrates NIR sample images.

probability of encountering phone usage. The dataset has been put together carefully in order to emulate real life conditions. Images were collected from the summer days, excluding the hours between 12:00 and 15:00 o'clock. On NIR and RGB images taken from this interval, inside of windshield cannot be seen due to excessive amount of reflection. Therefore, data from these hours are not included in test set. Figure 6 shows some of the challenging cases in which windshield detection or driver detection fails.

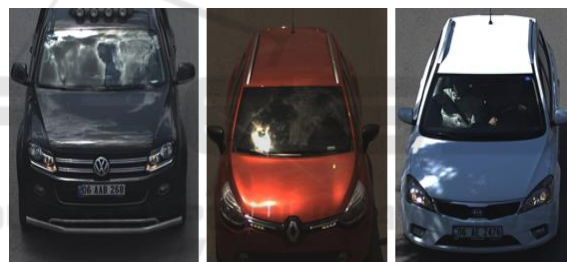


Figure 6: Samples of excessive amount of reflection on the windshield of vehicles.

4.3 Test Results

In our analysis, first, we would like to present the performance of the windshield detection and driver detection subtasks using test images. Detector output is considered as correct if its overlap with ground truth is greater than 80 %. On the test set, SSD detector achieves an accuracy of 99.5 % for windshield detection task. Once the windshield region is detected, the driver detector is applied to detect driver on the front seat. On the same test dataset, overall accuracy is measured as 99.3 %. Note that, 0.7 % loss does not only depend on the performance of the driver detector. It also depends on the performance of the windshield detector. These undetected windshield images causes additional loss to the driver detector, therefore performance of windshield detector affects the performance of driver detection.

Table 4: Confusion Matrix of proposed SSD method. Numbers in the table are presented as NIR and RGB test results, respectively.

Actual Class / Predicted Class (NIR/RGB)	Violation	No-Violation	Hard Negative	Overall
Violation	50/21	29/11	34/17	113/49
No-Violation	15/10	3269/2020	235/143	3519/2173
Hard Negative	8/4	35/15	42/23	85/42
Overall	73/35	3333/2046	311/183	3717/2264

When the driver is detected, we apply phone usage violation detection/classification methods for either NIR or RGB images. Table 2 presents the overall performance of the proposed methods for phone usage violation detection and Table 3 shows visual illustration obtained for SSD method under various imaging conditions.

Table 2: Accuracy Rates of the proposed methods.

Methods	SSD	CNN	FV
Accuracy (NIR/RGB)	0.904/ 0.911	0.739/ 0.720	0.641/ 0.881

Table 3: A visual illustration of SSD output for sample images. First, second and third column show no violation, violation and hard negative cases, respectively.



In order to compare the performance of SSD, we utilized image classification based CNN and FV models. It is clear that SSD outperforms CNN model and FV model by giving the highest accuracy. SSD is very successful at learning a pattern thanks to its spatial and spectral learning mechanism. For better interpretation of the performance, confusion matrix of results, sensitivity and precision rates of SSD method are shown in Table 4. We have partitioned our test set as NIR and RGB images in order to analyse the results of different image representation. The results demonstrate that usage of either NIR or RGB images is convenient for our phone usage violation detection task. Hard negative case detection allows us to

eliminate unnecessary violation detection in the driver region containing hand gestures.

According to the results, even though high accuracy rate is observed, sensitivity and precision rate is relatively low. Considering our NIR and RGB test set sensitivity rate of SSD model is 44, 2 % and 42, 8 %, respectively. In some cases, mobile phone use of driver may not be observed clearly. Therefore, detectors tend to decide as there is no violation and it causes serious reduction in sensitivity rate. From a different viewpoint, even though there is no violation in some cases, hand gestures of driver might cause a complexity making a right decision of detector. Therefore, For NIR and RGB images in the test set, precision rate drops to 68, 4 % and 60 %, respectively.

Computation times of the proposed methods are analyzed using a computer with 16 GB RAM, Intel Core i7 processor and an Nvidia GeForce GTX 780 Ti GPU card. GPU card is utilized for SSD object detection and CNN image classification tasks. It is observed that SSD300 model produce detection results at 60 milliseconds and CNN model classifies an image at approximately 32 milliseconds as shown in Table 5.

Table 5: Run-time of 3 methods for a single image.

	SSD	CNN	FV
Run Time (seconds)	0,060	0,032	0,078

5 CONCLUSION

In this study, we proposed driver cell phone usage violation detection using license plate recognition camera images. Proposed method combines state-of-the-art deep learning based object detection technique. In order to compare our deep learning based SSD model, we utilized deep learning based CNN model, also we analysed machine learning based FV method as a prior work. Proposed SSD model typically achieve an overall accuracy around 91 % on a test set consisting of 2264 RGB images and

3717 NIR images. In the future, we will look into using the combination of different deep learning based object classification techniques and well-known classification techniques.

REFERENCES

- IBM Smarter Cities Public Safety, (2012). Law Enforcement.
- European Road Safety Observatory (ERSO), (2015). *Cell phone use while driving*, https://ec.europa.eu/transport/road_safety/erso-synthesis-2015-cellphone-detail_en.pdf.
- World Health Organization (WHO), (2017). “*Save Lives-a Road Safety Technical Package*”, <http://www.who.int/>, 2017.
- Strategic Highway Research Program (SHRP2), (2006-2015). <http://www.trb.org/StrategicHighwayResearchProgram2SHRP2/Blank2.aspx>.
- Artan, Y., Bulan, O., Loce, R. P., Paul, P., (2014) Driver Cell Phone Usage Detection From HOV/HOTNIR Images, In *IEEE Conf. on Comp. Vis. Pat. Rec.*
- Berri, R. A., Silva, A. G., Parpinelli, R. S., Girardi, E., Arthur, R., (2014). A Pattern Recognition System for Detecting Use of Mobile Phones While Driving, In *arXiv:1408.0680v1*.
- Elings, J.W., (2018). Driver Handheld Cell Phone Usage Detection, *Utrecht Univ. M.S. Thesis*.
- Seshadri, K., Juefei-Xu, F., Pal, D. K., Savvides, M., Thor, C., (2015). Driver Cell Phone Usage Detection on Strategic Highway Research Program (shrp2) Face View Videos, In *Proc. IEEE Conf. CVPRW*, pp. 35-4.
- Le, T. H. N., Zheng, Y., Zhu, C., Luu, K. and Savvides, M., (2016). Multiple Scale Faster-RCNN Approach to Driver’s Cell-phone Usage and Hands on Steering Wheel Detection, in *CVPR*.
- Zhou, B., et al., (2017). Seat Belt Detection Using Convolutional Neural Network Bn-Alexnet, pp.384-395, in *ICIC*.
- Elihos, A., Balci, B., Alkan, B., Artan, Y., (2018). Comparison of Image Classification and Object Detection for Passenger Seat Belt Violation Detection Using NIR & RGB Surveillance Camera Images, in *AVSS*.
- Bojarski, M., Desta, D., Drawokovski, D., Firner, B., Flepp, B., Goyal, P., Jackel, L., Monfort, M., Muller, U., Zhang, J., Zhang, X., Zhao, J., Zieba, K., (2016). End-to-end deep learning for self driving cars, In arxiv Preprint arxiv:1604:07316.
- Liu, W., Anguelov, D., Erhan, D., Szegedy, C., Reed, S., Fu, C., Berg, A., (2016). Ssd: Single shot multibox detector, In European Conference on Computer Vision, pp. 21–37. Springer.
- Redmon, J., Divvala, S., Girshick, R., Farhadi, A., (2016). You only look once: Unified real time object detection, In *IEEE CVPR*, pp. 779-787.
- Ren, S., He, K., Girschick, R., (2015). Faster R-CNN: towards real-time object detection with region proposal networks, In *NIPS*.
- Huang, J., Rathod, V., Sun, C., Zhu, M., Korattika, A., Fathi, A., Fischer, I., Wojna, Z., Song, Y., Guadarrama, S., Murphy, K., (2017). Speed/accuracy trade-offs for modern convolutional object detectors, in arXiv: 1611.10012v3.
- Deng, J., Dong, W., Socher, R., Li, L., Li, K., Fei-Fei, L., (2009). Imagenet: A large-scale hierarchical image database, in *Proceedings of the IEEE Conference on Computer Vision and Pattern Recognition*, pp. 248–255.
- Simonyan, K., X Zisserman, V., (2014). Very Deep Convolutional Networks for Large-Scale Image Recognition, In arXiv:1409.1556.
- Perronnin, F., Sanchez, J., Mensink, T., (2010). “Improving Fisher Kernels for Large-Scale Image Classification,” in *ECCV*.
- Kingma, D. and J. Ba (2014). Adam: A method for stochastic optimization. arXiv preprint arXiv:1412.6980.
- Xiong, X. and Torr, F. De la, (2013). *Supervised Descent Method and its Application to Face Alignment*. In *IEEE Conference on Computer Vision and Pattern Recognition (CVPR)*, pages 532–539.
- Cortes, C., and Vapnik, V., (1995). *Support-Vector Networks*. *Machine Learning*, 20(3):273–297.
- Das, N., Ohn-Bar, E. and Trivedi, M.M , (2015). *On performance evaluation of driver hand detection algorithms: Challenges, dataset, and metrics*. In *Conf. on ITS*.
- Schapire, R.E and Singer, Y., (1999). Improved Boosting Algorithms Using Confidence-rated Predictions. *Machine Learning*, 37(3):297–336.